Meccanica (2016) 51:635–653
DOI 10.1007/s11012-015-0227-8

A two-step damage identification approach for beam structures based on wavelet transform and genetic algorithm

Seyed Alireza Ravanfar · Hashim Abdul Razak · Zubaidah Ismail · S. J. S. Hakim

Received: 9 November 2014 / Accepted: 17 June 2015 / Published online: 25 June 2015

Abstract A two-step damage identification approach based on wavelet multi-resolution analysis and genetic algorithm (GA) in beam structures is presented in this paper. The location of the crack is identified in the first step by defining the damage index called relative wavelet packet entropy. Then, the damage severities at the identified locations are assessed in the second step using GA. The wavelet packet component energies for each damage depth used in the first step and the severity evaluation database required for the second step to reveal the relationships between the energies and damage severities are obtained using a multi-resolution wavelet packet transform. The effects of wavelet type and decomposition level on the detection of damage location are examined in beams with various damage scenarios in the presence of different noise levels. To investigate the robustness and accuracy of the proposed method, numerical examples and experimental cases with different damage depths are considered. The results demonstrate that the proposed method performs reasonably well and has great potential in the identification of damage locations and estimation of damage severities.

Keywords Damage identification · Wavelet packet transform · Genetic algorithm · Wavelet type · Beams

S. A. Ravanfar · H. A. Razak (✉) · S. J. S. Hakim
StrucHMRS Group, Department of Civil Engineering, Faculty of Engineering, University of Malaya, 50603 Kuala Lumpur, Malaysia
e-mail: hashim@um.edu.my

S. A. Ravanfar
e-mail: r.ravanfar@gmail.com

S. J. S. Hakim
e-mail: hakim_civil@yahoo.com

Z. Ismail
Department of Civil Engineering, Faculty of Engineering, University of Malaya, 50603 Kuala Lumpur, Malaysia
e-mail: zu_ismail@um.edu.my

1 Introduction

During the service life of various civil, mechanical and aerospace structures, damage can accumulate, nucleate and propagate leading to out-of-service conditions, and, sometimes, dangerous collapses. Therefore, structural health monitoring (SHM) is an important tool for identifying the presence and the evolution of possible damage. In the last few decades, researchers have exerted great effort in developing different vibration responses based on damage identification methods [1–5] to replace traditional non-destructive techniques, such as acoustic, magnetic field, ultrasonic, eddy-current, radiograph, thermal field methods [6, 7], which suffer from weaknesses of requiring a priori knowledge of the damage location and its accessibility.

The fundamental theory for vibration response-based damage identification is that damage causes

changes in the physical properties i.e. stiffness, damping and mass by which the modal properties namely modal damping, mode shapes and natural frequencies will be subsequently affected. Hence, damage can be recognized by analyzing the variations of vibration characteristics of the structure. The vibration-based damage detection methods have received much attention in the past few decades, and several approaches have been suggested [2, 4].

Structural damage is typically a local phenomenon. Fourier analysis transforms the vibration signal from a time-based or space-based domain to a frequency-based one. So, it is sometimes impossible to determine when or where a particular event takes place by using Fourier transforms (FT). To overcome this deficiency, the short-time Fourier transform (STFT) that was proposed by Gabor [8] can be used. This windowing technique analyzes only a small section of the signal at a time. The STFT maps a signal into a 2-D function of time or space and frequency. The transformation has the disadvantage that the information about time or space and frequency can be obtained with limited precision that is determined by the size of the window. A higher resolution in both time and frequency domain cannot be achieved simultaneously since once the window size is fixed, it is the same for all frequencies.

Among the recent vibration-based structural damage detection techniques, wavelet analysis has been widely recognized as an effective and robust damage detection tool because of its capability to deal with non-stationary signals and to localize singularities in a function or in any of its derivatives [9–11]. Wavelet functions are included in the family of basis functions that are capable of depicting a signal in a localized frequency (or scale) and time (or space) domain. The main advantage obtained by using wavelets is the capability to execute local analysis of a signal, i.e. zooming in on any interval of space or time. Wavelet analysis is capable of demonstrating some hidden features of the data that conventional Fourier analysis fails to detect. The wavelet-based techniques can be classified into two categories: wavelet transform (WT)-based approach and wavelet packet transform (WPT)-based approach.

According to different functions of WT, as the first approach, damage can be found by variations in the WT coefficients that are associated with the undamaged and damaged state. Melhem and Kim [12, 13] employed this method to identify the location of cracks in a beam. The second kind of WT-based approach detects the damage by a combination of wave propagation theory and WT. Analyzing the measured responses and locating wavelet coefficient peaks are initially carried out, which facilitates the shortest path arrival time of flexural waves caused by damage to be estimated, which is then followed by localizing or quantifying the damage. Salehian et al. [14] determined the location of the applied load, and modeled the structural damage by establishing a set of nonlinear equations to solve this inverse problem.

The third kind of approach takes advantage of the modulus maximum line of continuous wavelet transform (CWT) coefficients or the detailed signals of discrete wavelet transform (DWT) to identify, localize or quantify damage through detection of the discontinuities of structural responses. In fact, this category assumes that the presence of damage introduces discontinuities in structural responses at the sites of damage. Even though the signal to be processed by the CWT is frequently the mode shape of the damaged structure [15–26], Wang and Deng [27] employed other spatial data like the displacement and strain measurements of a cracked beam subjected to impact loading to locate damage by sensing local perturbations at the sites of damage, and then considering the displacement response of a plate under in-plane stress. Umesha et al. [28] proposed a new method based on the CWT to detect the location and also to quantify the crack using the deflection response of the damaged beams.

Despite the effectiveness of wavelet analysis in damage identification, the reliable detection of tiny damages is still an open challenge because they can be masked by measurement noise and/or edge (border) distortion of the WT. In addition, acquiring modal shapes in practice usually involves installing a large number of sensors that is not always straightforward or practical. In addition, this affects the structural/vibrational properties [29].

According to the above discussion, the WPT-based approach, which is a generalized form of the DWT is proposed here to present the detailed information of signals in the high-frequency region. The WPT creates the same frequency bandwidths in every resolution. Such features of the wavelet are naturally inherited by the wavelet energy and entropy, leading to better damage identification. Several researchers took the wavelet packet component energies extracted from

structural dynamic responses as a characteristic feature, and established neural networks to detect the occurrence of damage, location and damage severity [30–34].

The wavelet entropy, which is a combination of entropy and wavelet, could take advantage of both methods to explain the characteristics of a signal, which are not directly visible in the original space. The wavelet entropy is modified to give a damage signature, which can both be achieved at different time stations and spatial locations to identify the existence of damage [35, 36]. Lee et al. [37] proposed a new damage detection algorithm based on the continuous relative wavelet entropy (CRWE) for truss bridge structures. The damage-sensitive index (DSI) of each sensor's location was defined by CRWE measurements of different sensor-to-sensor pairs. The CRWE was reported to be able to detect damage but with considerably large computation cost for the real time monitoring algorithm. In particular, Ren and Sun [38] suggested a combination of information entropy [39] and DWT having a damage-sensitive feature to characterize the level of irregularity in the measured signals to identify the occurrence and location of damage in beam structures.

Previous studies used a combination of DWT and Shannon entropy to generally identify the occurrence and location of damage [38, 39]. However, they are not effective for estimating the location of small-scale damage in various positions due to the application of only one specified mother wavelet function and decomposition level, while the robustness of wavelet-based techniques are absolutely dependent on the mother wavelet function to identify the damage location, especially in multi-damage scenarios. In addition, wavelet-based methods are not always reliable in the prediction of damage severities. Therefore, computational intelligence methods, such as genetic algorithms (GAs) have been applied to overcome this difficulty.

The GAs have been recognized as promising intelligent search techniques for difficult optimization problems and more attention has been given to the design of an effective damage detection procedure [40–44]. Hao and Xia [45] applied a GA with real number encoding to identify the structural damage by minimizing the objective function, which directly compares the changes in the measurements before and after damage. Three different criteria were considered, namely, the frequency changes, the mode shape changes, and a combination of the two. The algorithm did not require an accurate analytical model and gave better damage detection results for the beam than the conventional optimization method. Vakil-Baghmisheh et al. [46] successfully applied the GA to predict the size and location of a crack in a cantilever beam by minimizing the cost function, which was based on the difference in the measured and calculated natural frequencies.

In this paper, a two-step vibration-based damage detection method is presented in the framework of the wavelet multi-resolution analysis (MRA) and optimization techniques. In the first step, the multi-resolution WPT is combined with entropy analysis to determine an effective damage indicator, relative wavelet packet entropy (RWPE), to obtain the information about the relative energy correlated with various frequency bands presented in structural response segments for investigating the location of damage. To improve the detection accuracy of identifying small-scale damages with different depths in various locations, several types of wavelet function and decomposition levels are examined. In the second step, the GA optimization method was applied to estimate the damage severities by defining a database to reveal the relationships between the energies obtained in the first step and damage severities. Both numerical simulation and experimental data with different damage scenarios revealed that the proposed algorithm has great potential in damage identification in beam-like structures and that it is insensitive to measurement noise.

2 Wavelet multi-resolution analysis

The MRA of wavelet is a significant property in the multilevel approximation of engineering problems [47]. The concept of MRA for square-integrable signals in the context of wavelet analysis was elaborated upon by Mallet [48]. The MRA can decompose a signal into components spanned by the scaling and wavelet basis functions at different resolutions. Any finite energy function $f(t)$ can be expressed by:

$$f(t) = \sum_{k=-\infty}^{\infty} a(j_o,k)\varnothing_{j_o,k}(t) + \sum_{j=j_o}^{\infty}\sum_{k=-\infty}^{\infty} d(j,k)\psi_{j,k}(t) \quad (1)$$

where $\varnothing_{j_o,k}(t) = 2^{-j_0/2}\varnothing(2^{-j_o}t - k)$ and $\psi_{j,k}(t) = 2^{-j/2}\psi(2^{-j}t - k)$ are the scaled and translated version of the scaling function $\varnothing(t)$ and mother wavelet $\psi(t)$, respectively, $a(j_o, k)$ is the *kth* approximation at the scale index j_o and $d(i, k)$ is the *kth* detail coefficient at scale index j. In Eq. (1), the first summation gives a low resolution or coarse approximation of $f(t)$ at the scale index j_o. For each j in the second summation, a higher or finer resolution function that included more detail of $f(t)$ is added. Equation (1) can be simplified as:

$$f(t) = A_{j_o} + \sum_{j=j_o}^{\infty} D_j \tag{2}$$

where:

$$A_{j_o} = \sum_{k=-\infty}^{\infty} a(j_o, k)\varnothing_{j_o,k}(t) \tag{3}$$

is the approximation at level j_o and:

$$D_j = \sum_{k=-\infty}^{\infty} d(j, k)\psi_{j,k}(t) \tag{4}$$

is the detail at level j. The scaling function $\varnothing$ satisfies the scaling condition:

$$\varnothing(t) = \sum_{k\in\mathbb{Z}} c(k)\varnothing(2t - k) \tag{5}$$

where Eq. (5) is called the two-scale relation for the scaling function $\varnothing(t)$ and $\{c(k)\}_{k\in\mathbb{Z}}$ are the coefficients for this relation. Generally, the MRA proposes that the scaling function plays a key role in the piecewise approximation of the continuous function $f(t)$ and depending on the scaling index. In addition, based on such a scaling function $\varnothing$ a mother wavelet ψ can be created as:

$$\psi(t) = \sum_{k\in\mathbb{Z}} b(k)\varnothing(2t - k) \tag{6}$$

where $b(k)$ are the coefficients for the two scale relation for the wavelet function $\psi(t)$. Note that the MRA is not unique and relies on the selection of the mother wavelet function. The selection of the mother wavelet and scaling function is application-dependent; therefore, no specific selection of the mother wavelet and scaling function can be employed for all applications with the desired results. In this study, Daubechies wavelets from the orthogonal wavelets family are employed, since they have been widely implemented in vibration signals. Also, the order of the mother wavelet function is the main issue in the wavelet analysis, which is determined by trial-and-error based on the intrinsic properties of the data [10, 38, 49–52].

3 Wavelet packet transform

Wavelet analysis is MRA in the time and frequency domain of a non-stationary signal. It can be considered as an extension of the traditional FT with a modifiable window size and location [53]. WPT can be considered as an extension of the DWT, which does not require a priori knowledge of the frequency bands (i.e. scales) but it filter the signal in adaptive way. The difference between WPT and DWT is that, the WPT decompose not only the approximation but also the detail coefficients at each level of decomposition. Therefore it is more flexible and have wider base for the analysis of signals. The idea of separating the signal into packets is to obtain an adaptive partitioning of the time frequency plane depending on the particular signal. More details can be found in the textbook by Mallat [54]. The wavelet packet function is defined as:

$$\psi^i_{j,k}(t) = 2^{-j/2}\psi^i\left(2^{-j}t - k\right) \quad i = 0, 1, 2, \ldots, 2^j - 1 \tag{7}$$

where a wavelet packet $\psi^i_{j,k}(t)$ is a function of three indices with integers *i, j* and *k*, denoting the modulation, the scale and the translation parameter, respectively. Moreover, $\psi^0(t) = \varnothing(t)$ for $i = 0$ and $\psi^1(t) = \psi(t)$ for $i = 1$. The wavelet $\varnothing(t)$ is called the scaling function and $\psi(t)$ called the mother wavelet function. The wavelets ψ^i for $i > 1$ are obtained from the scaling function and the mother wavelet function as:

$$\psi^{2i} = \sqrt{2}\sum_k h(k)\psi^i(2t - k) \tag{8}$$

$$\psi^{2i+1} = \sqrt{2}\sum_k g(k)\psi^i(2t - k) \tag{9}$$

where g(k) and h(k) are quadrature mirror filters associated with the mother wavelet function and the scaling function. The signal is passed through a serious

of high pass filters, i.e. g(k), to analyze the high frequency, and through a serious of low pass filters, i.e. h(k), to analyze the low frequency. Hence, the original signal can be filtered in different frequency bands. In this work, the measured dynamic structural response is decomposed into wavelet component functions. While the level of decomposition is j, 2^j WPD components can be obtained.

The original signal can be expressed as a summation of WPD components as:

$$f(t) = \sum_{i=1}^{2^j} f_j^i(t) \tag{10}$$

where t is time lag; $f_j^i(t)$ is the WPD component signal that can be represented by a linear combination of wavelet packet functions, as follows:

$$f_j^i(t) = \sum_{k=-\infty}^{\infty} C_{j,k}^i \psi_{j,k}^i(t) \tag{11}$$

where $C_{j,k}^i$ is the wavelet packet coefficient and can be calculated from:

$$C_{j,k}^i = \int_{-\infty}^{\infty} f(t)\psi_{j,k}^i(t)dt \tag{12}$$

WPT offers good time resolution in the high-frequency range of a signal and good frequency resolution in the low-frequency range of the signal.

4 Damage identification approach

Vibration-based structural damage identification is aimed at comparing structural parameters extracted from measured vibration signals between the undamaged and damaged state. When structural damage occurs, a corresponding change is produced according to the damage features that evolve from the structural response signals before and after the damage. The key issue in structural damage identification is how to identify and quantify this change. Therefore, this study deals with the development of a hybrid approach using RWPE and GA by defining a database to accurately determine the location and severity of the damage in beam structures. This approach contains two steps, i.e. the first is detecting damage locations and the second is to determine the severity of damage. In addition, to evaluate the influence of changing the wavelet function and level of decomposition on the accuracy of identifying damage location, the wavelet functions DB1 to DB10 are used for beams.

4.1 Damage location detection

To examine the structural health condition, it is essential to achieve an index that is sensitive to structural damage. Usually, the measured vibration signals are decomposed by WPT into component signals and then component energies are calculated. The wavelet packet component energy is a suitable tool for identifying and characterizing a specific phenomenon of signal in the time-frequency domain. It has been shown by Yen and Lin [55] that the energy stored in a specific frequency band at a certain level of WPD provides a greater potential for signal feature than the coefficients alone. Sun and Chang [52] conducted a comparative study on the sensitivity of four damage indices based on variations of frequency, mode shape, flexibility and wavelet packet energy, and deduced that the wavelet packet energy based index has a high potential to capture the reduction in structural stiffness. The sensitivity of the WPT component energy with regard to local change in the system parameters was derived by Law et al. [56]. Ren et al. [57] studied the application of the wavelet packet energy variation based damage detection method in bridge shear connector monitoring.

The wavelet packet energy E_f of a signal is defined as:

$$\begin{aligned} E_f &= \int_{-\infty}^{\infty} f^2(t)dt \\ &= \sum_{m_1=1}^{2^j}\sum_{m_2=1}^{2^j}\int_{-\infty}^{\infty} f_j^{m_1}(t)f_j^{m_2}(t)dt \end{aligned} \tag{13}$$

where $f_j^{m_1}$ and $f_j^{m_2}$ stand for decomposed wavelet components. The total signal energy can be expressed as the summation of wavelet packet component energies when the mother wavelet is orthogonal:

$$E_f = \sum_{i}^{2^j} E_{f_j^i} = \sum_{i=1}^{2^j}\int_{-\infty}^{\infty} f_j^i(t)^2 dt \tag{14}$$

Then, the energy ratio of each wavelet coefficient can be written as:

$$p_{ij} = \frac{E_{f_j^i}}{E_f} \tag{15}$$

The p_{ij} values correspond to a ratio of the energy of a particular coefficient $E_{f_j^i}$ to the total energy. The p_{ij} value acts like a probability distribution of the energy, therefore, the p_{ij} values sum to one.

The Shannon entropy represents the amount of information, which is also often used as a measure of the extent of signal energy concentration in the time-frequency domain. Ren and Sun [38] applied the concept of the wavelet entropy to structural damage detection problems. The wavelet entropy spectra represent the level of order/disorder of vibration signals [39].

The damage detection problem can be formulated through the changes in the wavelet packet entropy before and after the occurrence of damage. To identify the change in vibration signal p from a (potentially) damaged structure relative to the vibration signal q from an undamaged structure, the RWPE is defined as:

$$S^k_{RWPE}\left(p^k|q^k\right) = \sum_j \sum_i \left| p^k_{ij} ln\left(\frac{p^k_{ij}}{q^k_{ij}}\right)\right| \quad k = x, y, z \tag{16}$$

It is notable that accelerations measured in the same direction should be used in computations of RWPE. Since damage at a location affects the vibration signals in every direction, the damage index based on the RWPE is considered as:

$$DI_{RWPE} = \sum_{k=1}^{x,y,z} S^k_{RWPE}\left(p^k|q^k\right) \tag{17}$$

However, when the structure is damaged, the values of p_{ij} and q_{ij} become different, and, consequently, the RWPE value increases. The capability of RWPE-based structural damage identification to extract the irregular information of a signal due to damage is enhanced by its WPT component energy. The RWPE has significant usefulness at high frequency where the information of a high frequency level is important.

5 Numerical simulation

To validate the feasibility of the method proposed in this study, numerical simulation of four steel-I beams with material properties tabulated in Table 1 and various predetermined damage conditions is carried out, as demonstrated in Fig. 1. Beam 0 is considered as the reference beam without damage while beam 1 is the single damage scenario with damage located at point 5. Beam 2 has two points of damage at locations 11 and 13, and beam 3 has three points of damage at different locations 9, 11 and 13. Damage is simulated in the form of a notch with a width of 3 mm. Let t^d_n stand for damage depth in which n is a number assigned to each damage depth case (n = 1, 2, …, 25). The damage depth is increased gradually for all beams from 3 up to 75 mm, as depicted in Fig. 1a, to obtain the damage severity α_n calculated by Eq. (18):

$$\alpha_n = \frac{t^d_n}{t} \tag{18}$$

The time history acceleration responses of beams are computed by the finite element analysis package (ABAQUS) using transient dynamic analysis. To simulate an impulse load, the force-time history is applied at location 14 on the beam. This location is not a node point for the first five flexural mode shapes. If a node point of a mode shape is situated at the excitation point, then this mode cannot be excited and identified. Location 15 is very close to the support and can be affected by the support, thus it cannot be chosen as the excitation point. Also, locations 10, 11 and 13 have node points of modes 5, 3 and 4, respectively. Hence these nodes were eliminated to be chosen as excitation point as well. Therefore, location 14 was chosen against locations 8 and 12 for the following reasons: (1) Mid-span of beam is the node point for modes 2 and 4 and location 8 is located at the mid-span; (2) The damage locations in beam B3 are very close to location 12 and cannot be chosen as the excitation point. Thus, to provide a better excitation, location 14 was chosen as an excitation point in this study. The node acceleration responses of the beam under the

Table 1 Structural model parameters

Parameters	Value
Mass density (ρ)	7850 kg/m^3
Poisson's ratio (υ)	0.33
Elasticity modulus (E)	2.1 GPa
Length (L)	3 m

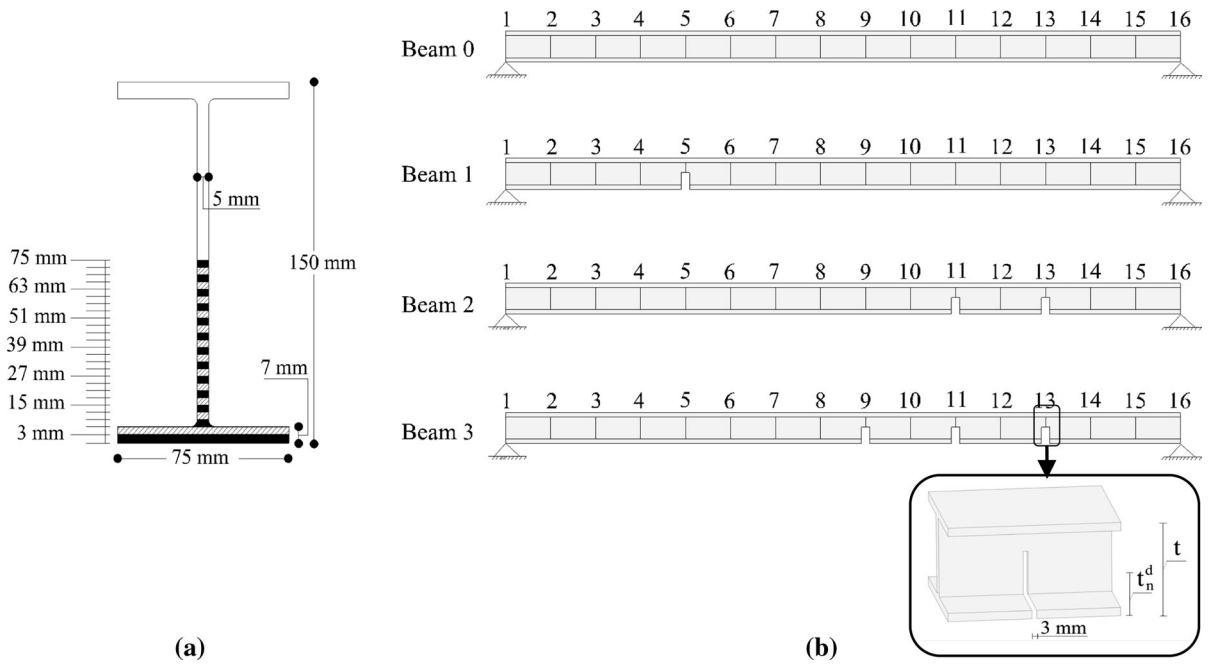

Fig. 1 I-section specimen. **a** Dimension and damage depth of beams, **b** damage location of beams

impulse load are obtained from sixteen locations on the top flange, as shown in Fig. 1b at a sampling frequency of 2000 Hz to identify the characteristics of damage in beams. Also, the frequency bands of the WPT components at decomposition level 6, as well as the relation between the WPT components and the frequencies of beam 0 are demonstrated in Table 2.

5.1 Identification of damage locations

To validate the proposed damage identification method, the simulated simply supported beams with damage elements are considered. The RWPE at 16 locations are calculated for each damage scenario based on Eq. (17), as shown in Fig. 2. According to these figures, the value and distribution of RWPEs changed considerably after damage. In cases with small damage, there is not much frequency difference in signals. This highlights that the type of mother wavelet and decomposition level play a key role in damage identification. Hence, in the single damage scenario, several wavelet functions and different levels of decomposition are investigated. More accurate results for these cases are obtained when the wavelet function DB2 and decomposition level 5 are used for differentiating the damages, as shown in Fig. 2a. The damage location can be clearly identified with the significant change in values of RWPE at location 5. However, the peak values of RWPE of the multiple-damage scenario for beam 2, where the damages are located at points 11 and 13, are identified by using the DB5 and decomposition level 6, as shown in Fig. 2b. The damage index is noticeably greater at point 11. Furthermore, in beam 3, DB10 with 6 levels of decomposition is found to be the appropriate DB order for damage identification. Figure 2c depicts that the peak value of the RWPE at point 9 is larger than that of point 11 and point 13.

In order to indicate the influence of changing the wavelet function on the accuracy of identifying the damage location, various wavelet functions DB1 to DB10 are applied for the considered beams. The standard difference percentage of RWPE $([(\sum \mathrm{RWPE}^{\max} - \sum \mathrm{RWPE}^{\mathrm{ave}})/(\sum \mathrm{RWPE}^{\mathrm{ave}})] \times 100)$ for each damage scenario at every specific depth of damage is calculated, as shown in Fig. 3. For beam 1, the standard difference percentage is obtained in decomposition level 5, as illustrated in Fig. 3a. A comparison of the histograms associated with every depth of damage for all considered DBs indicates that wavelet function DB2 is the suitable wavelet function order. However, in beam 2, as shown in Fig. 3b, the values of DB5 with 6 levels of decomposition are

Table 2 Frequency bands of the WPT Components at decomposition level 6 of beam 0

The sequence of WPT	Frequency bands of WPT components (Hz)	Natural frequencies (Hz)
1	[0–15.625]	12.888
2	[15.625–31.25]	25.784
3	[31.25–46.875]	–
4	[46.875–62.5]	52.80
⋮	⋮	⋮
15	[187.5–203.125]	201.64
⋮	⋮	⋮
28	[421.875–437.5]	429.67
⋮	⋮	⋮
48	[703.125–718.75]	714.90
⋮	⋮	⋮
64	[984.375–1000]	–

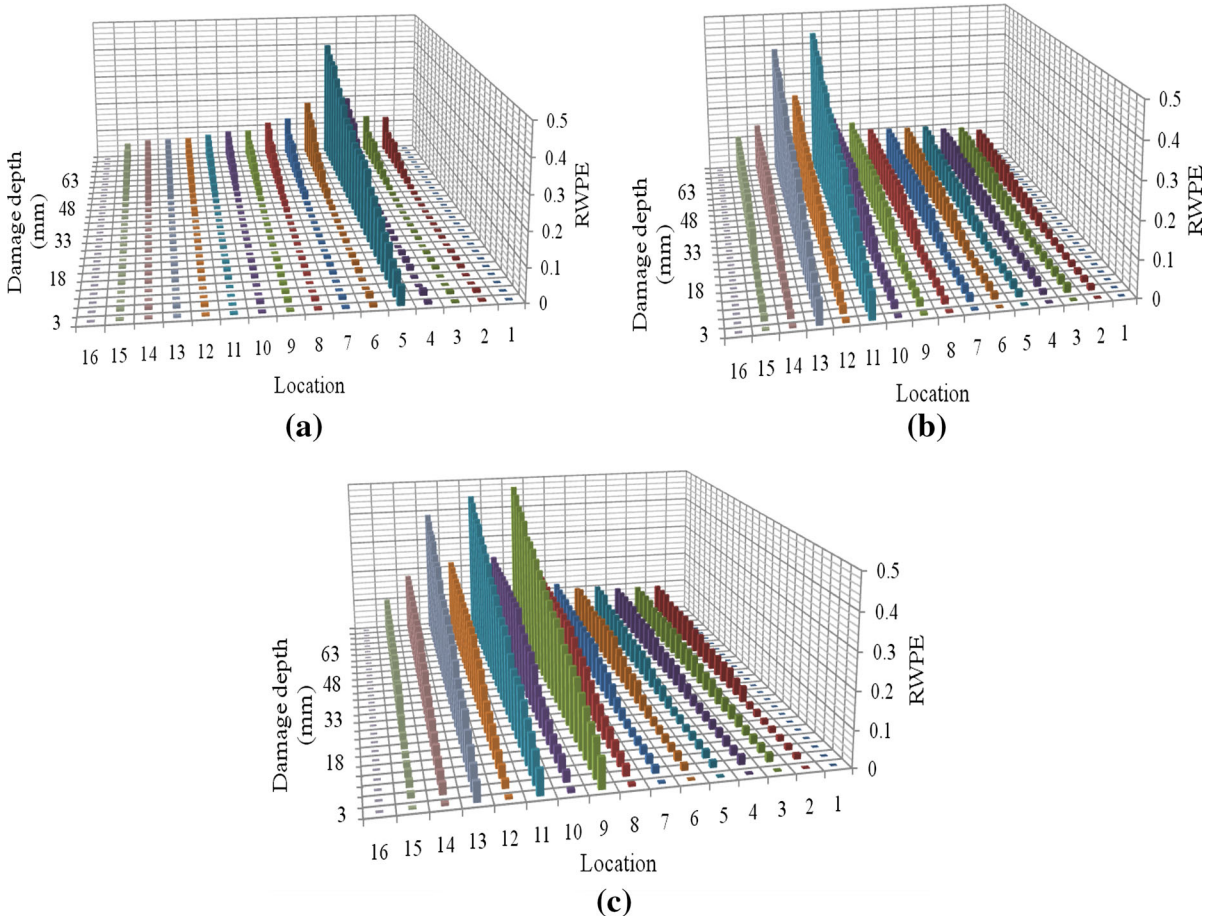

Fig. 2 The values of RWPE for each depth of damage. **a** Beam 1, **b** beam 2, **c** beam 3

larger than those of the other DBs. The results for beam 3 with multiple damages, as depicted in Fig. 3c, reveal that DB10 and the decomposition level of 6 can precisely identify the damage locations along the beam length compared with other Daubechies wavelet functions.

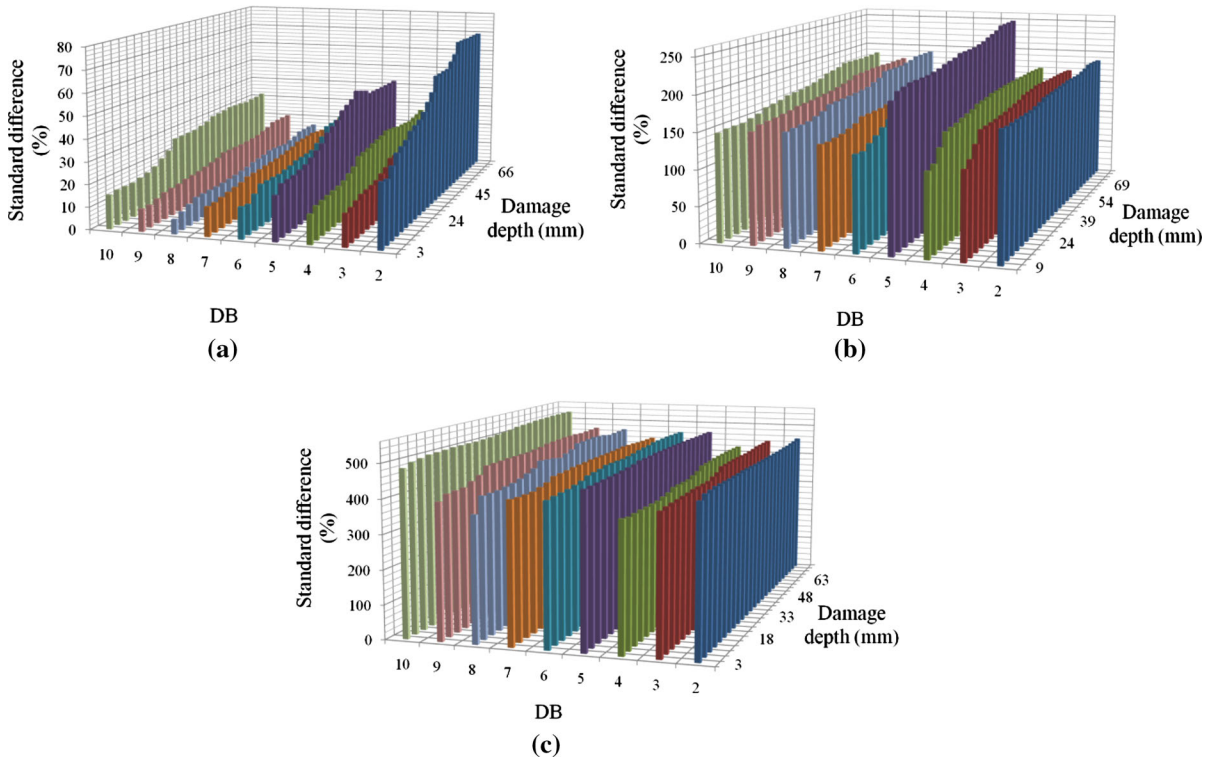

Fig. 3 Damage identification results using different wavelet function. **a** Beam 1, **b** beam 2, **c** beam 3

In addition, Fig. 4 depicts the values of RWPE in beam 2 to demonstrate the difference between various orders of Daubechies wavelets in discrimination of damage locations. Evidently, the damage locations were distinguishable in these histograms with RWPE reaching a maximum value at locations 11 and 13 which were the exact damage locations. By comparing the considered Daubechies orders shown in Fig. 4, it can be seen that the peak of RWPE was not as clearly distinguishable in DB6 even though it had the same location and severity of damages. Furthermore, DB5 showed a significant difference in the values of RWPE relative to the other DBs for each depth of damage. For DB2, the shortcomings were identical to that of DB6 but produced more accurate results. DB10 was not a worthy consideration since it was not able to precisely indicate the damage location. It is considerable to note that the accuracy of differentiating the damage cannot be compared to DB5 for the two damage scenario.

From the above observations, it may be construed that an increase in the damage depth of beams influences the vibration response signal, and, consequently, the RWPE values. Comparison of the peak values of RWPEs in the region of damage reveals that larger values of the RWPE take place when the damage is located near the center of the beam since the local perturbations caused by the damage occur at a far distance from the support. On the other hand, the presence of damage adjacent to the support results in a singularity around the support, which cannot be found with a predetermined DB. The problem with one predetermined DB arises when multiple damages are located on the beam and the proper selection of the mother wavelet function influences the accuracy of damage location identification.

Therefore, the selection of a proper mother wavelet for wavelet-based methods is important, as it can affect the performance improvement of the proposed method in order to achieve accurate results. The type of mother wavelet function plays a key role in reducing the false positives adjacent to the damage locations, as depicted in Figs. 3 and 4. This is mostly because the correlation between the mother wavelet

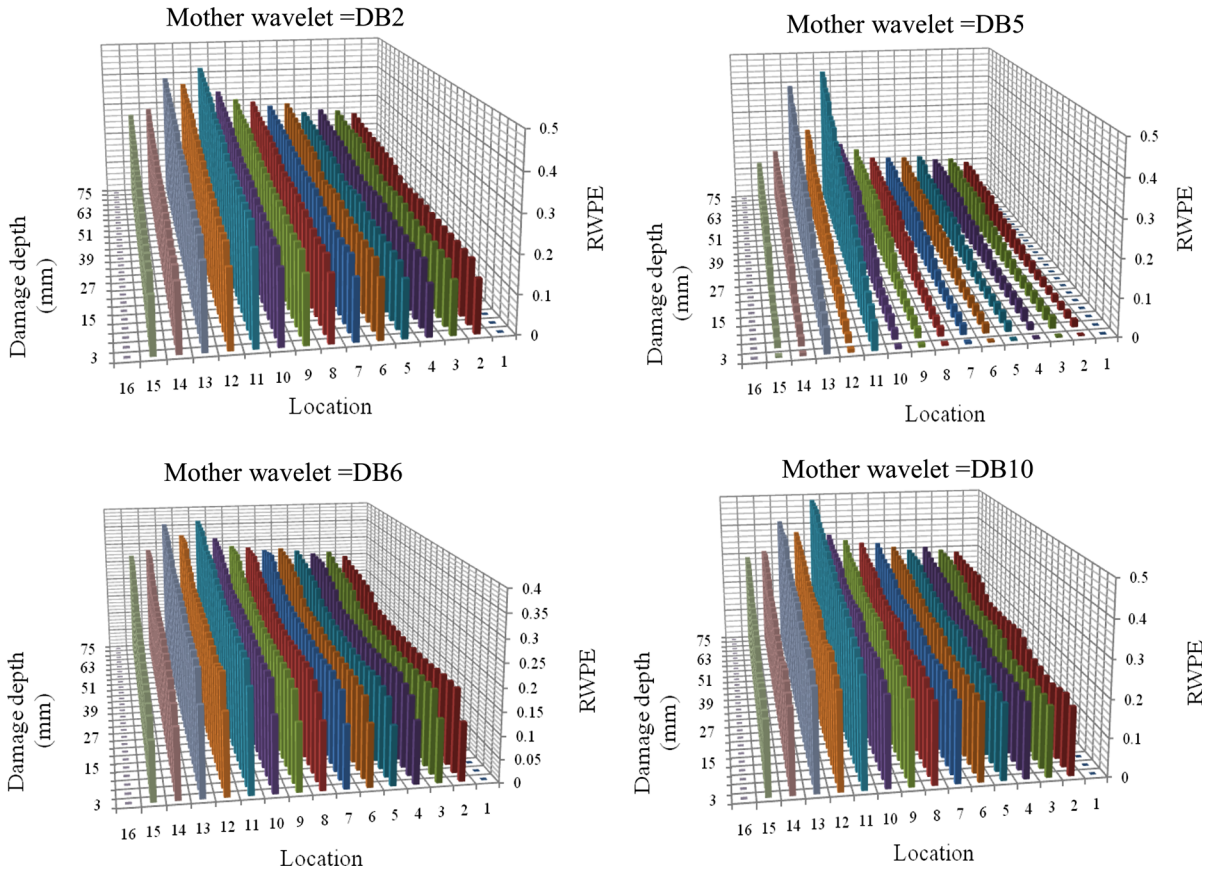

Fig. 4 Histograms of RWPE in beam 2 with different orders of Daubechies wavelets

functions and the signal is calculated as a wavelet coefficient.

5.2 Verification of noise effect on the proposed method

The presence of noise in the recorded signal is unavoidable in real life applications. Therefore, to investigate the effect of measurement noise on the performance of the proposed method, white Gaussian noise (WGN) is added to the generated acceleration signals of the test cases to simulate the uncertainties of real-life problems such as the environmental conditions during an experimental work. The noise intensity is defined by the signal-to-noise ratio (SNR):

$$\mathrm{SNR(dB)} = 20\log_{10}\frac{A_S}{A_N} \tag{19}$$

where A_S and A_N are the root-mean-square (RMS) value of the acceleration signal and the noise, respectively. In present applications, the effect of different levels of noise on damage identification is investigated by applying SNRs 2, 5 and 10 dB. Figure 5 shows the noise-contaminated original acceleration signals at location 8 for the undamaged case.

Beam 3 with three damage scenarios is analyzed for noise effect, and the identified results in terms of the noise levels are shown in Fig. 6. It can be observed that the presence of noise did not have an adverse effect on the histograms regardless of noise level and that the RWPE values are identical to the noiseless case. This could because the noise is assigned to the different wavelet functions and the noise effect in each bandwidth is reduced. Hence, it can be inferred that the proposed method will work satisfactorily in the presence of measurement noise.

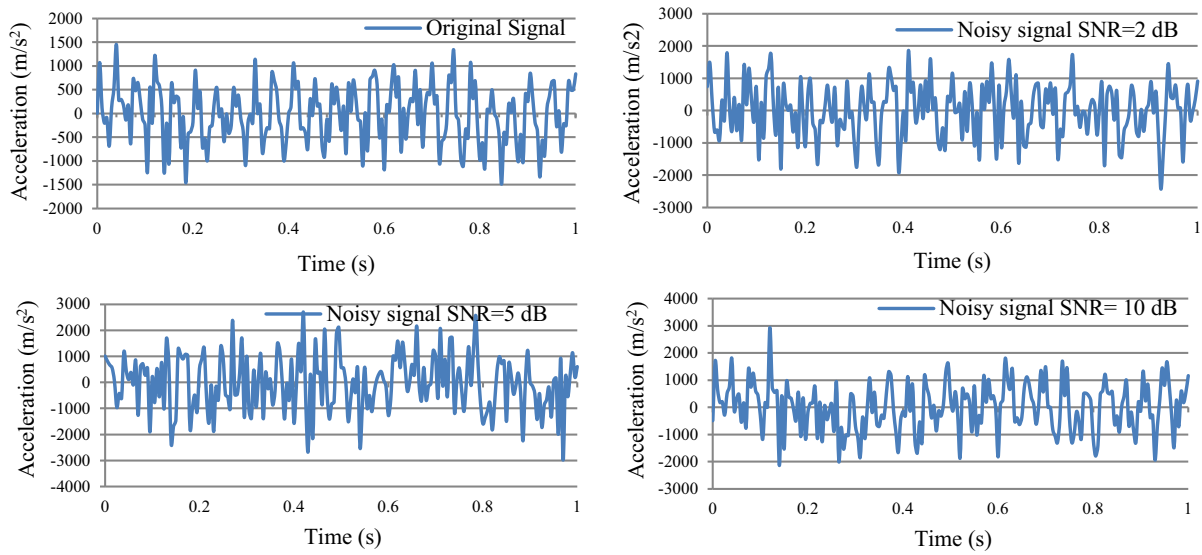

Fig. 5 Different levels of noise contamination in the measured signal at location 8 for the undamaged case

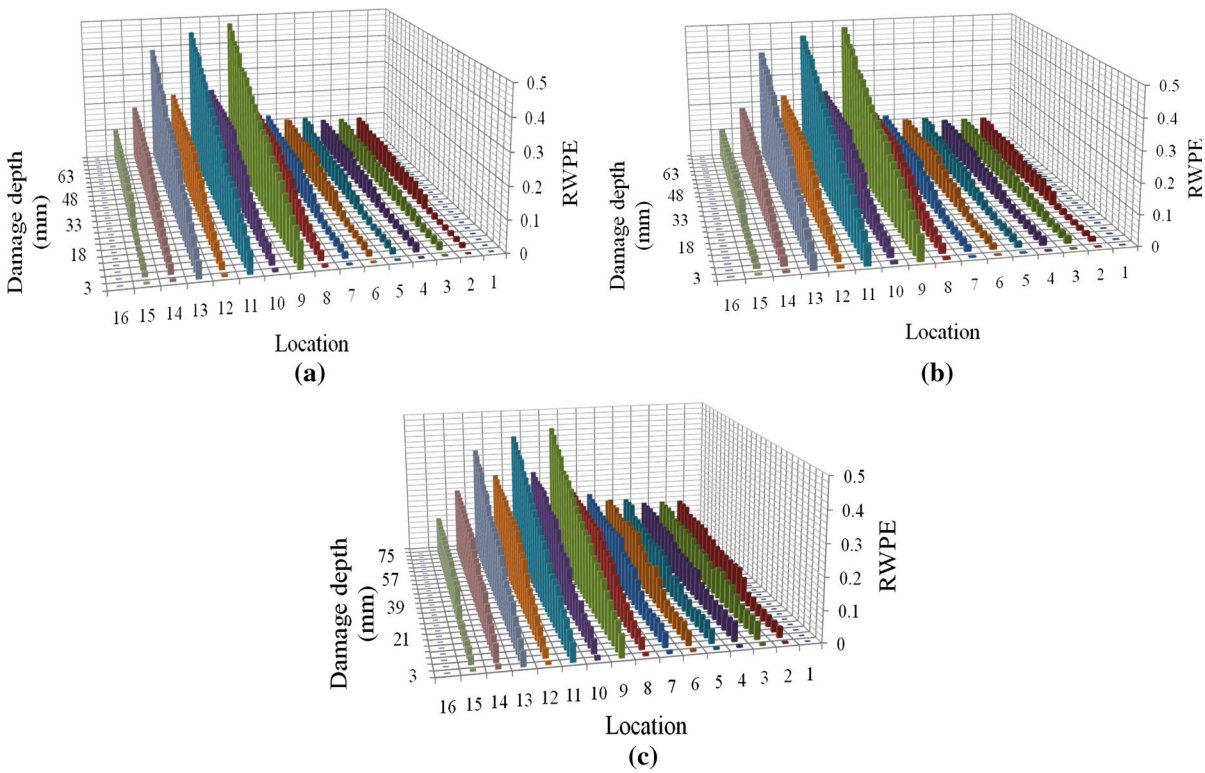

Fig. 6 Damage identification results in beam 3 after adding different levels of noise. **a** SNR = 2 dB, **b** SNR = 5 dB, **c** SNR = 10 dB

6 Evaluation of damage severities

6.1 Genetic algorithm

GAs are stochastic search algorithms, which are based on the mechanics of natural selection and natural genetics, which is designed to efficiently search large, non-linear, discrete and poorly understood search spaces, where expert knowledge is scarce or difficult to model and where traditional optimization techniques fail [58]. Typically, a simple GA consists of three operations: (1) parent selection, (2) crossover, and (3) mutation.

In this research, a population of individuals is created by randomly generating a set of candidate solutions and encoding these solutions into binary strings. Each individual in the population then undergoes evaluation and is assigned a fitness value based on how well the individual satisfies the stated objective. Tournament selection is used to pick individuals to undergo crossover and mutation. The two-point crossover is employed for every chromosome of the chromosome-pair with a 50 % probability of selection; the two parents selected for crossover are in charge of exchanging information that lies between two randomly generated points within the binary string. The chromosomes are the representations of tentative solutions, which can be evaluated by a fitness function. The fitness function determines the fitness of the chromosome. These chromosomes undergo

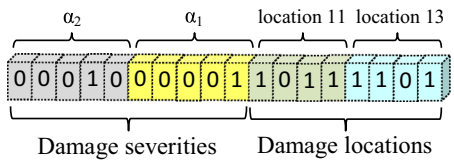

Fig. 7 Proposed chromosome for GA for two damage location and severities

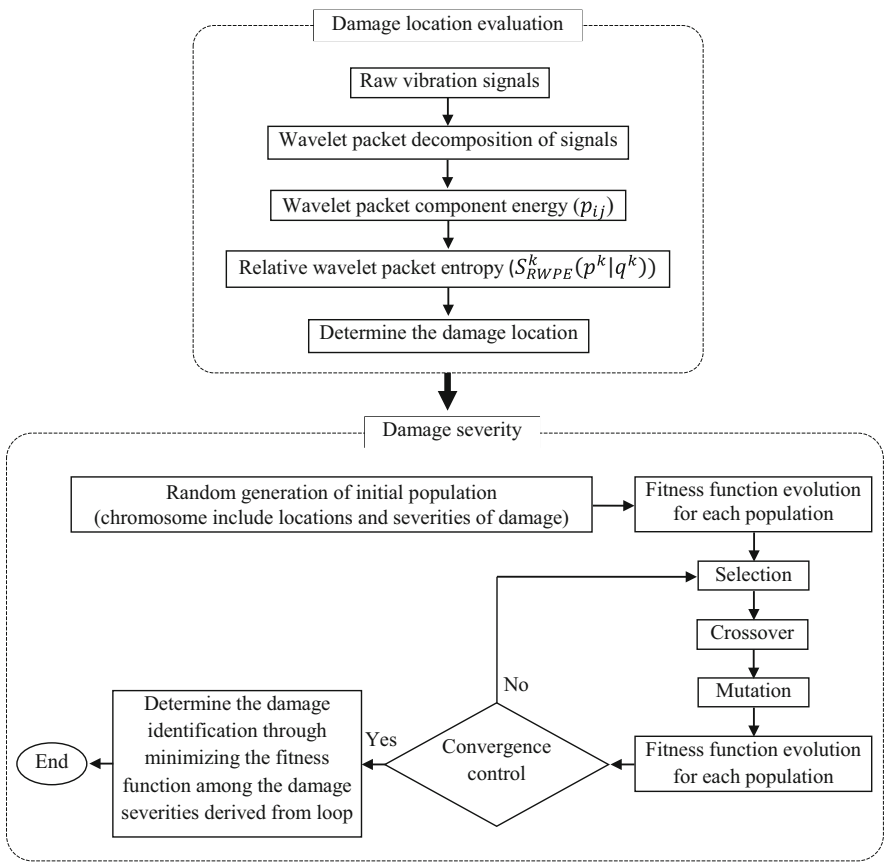

Fig. 8 Flowchart of the entire proposed algorithm

Table 3 GA set up parameters

Number of generation	500
Population	100
Selection function	Tournament
Fitness normalization	Rank
Crossover	Pc = 0.7, two-point, uniform
Mutation	Pm = 0.05, uniform

genetic operations to produce next-generation chromosomes. This occurs repeatedly until chromosomes of acceptable solutions are discovered.

The selected chromosome has two kinds of variable: the damage locations, and severities of damage. The GAs use bit strings to represent their chromosomes. Consequently, each gene of the chromosome may be either 0 or 1. Therefore, bit strings may be directly used to encode the candidate solution. In other words, the solution for the true damage configuration is a bit string whose substrings indicate the related parameters. Figure 7 depicts the proposed chromosome in a case with two damage locations with different severities.

In order to formulate the damage severities problem as an optimization problem, the following fitness function is applied to search for the "best fit" severities from the evaluation database:

$$\min f = \left\| \frac{\sum_{k=1}^{nd} F_{\alpha k}^{\beta k} - F_m}{\sum_{k=1}^{nd} F_{\alpha k}^{\beta k}} \right\|_2 \tag{20}$$

where $\|\cdot\|_2$ is the Euclidean norm, $F = \sum_j \sum_j p_{ij}(\alpha_1, \alpha_2, \ldots, \alpha_n)$ is the discrete function of the damage severities $\alpha_n (n = 1, 2, \ldots, 25)$ at sixteen locations (it is reflected by the severity evaluation database), constraint $0.02 < \alpha_n < 0.5$ limits the severity search space from 0.02 to 0.5, k is the number of damage locations, β is the sensor locations and F_m is the summation of measured energies in damage locations for each severity of damage. For the purpose of simulation, only the noise-contaminated signals calculated by Eq. (19) are employed to obtain energies in each frequency band.

To sum up, GA is used to optimally search locations and severities of damage, which can be reflected by the values of the energies. Figure 8 depicts the whole scheme of the damage identification algorithm. Some preliminary tests are performed to decide the GA set up parameters. The nal set up parameters used ithis work are shown in Table 3.

Table 4 Considered damage cases in beams

Case	Damage severity					
	Beam 1	Beam 2		Beam 3		
	α_1	α_1	α_2	α_1	α_2	α_3
1	0.02	0.02	0.02	0.02	0.04	0.02
2	0.04	0.1	0.4	0.08	0.02	0.48
3	0.1	0.06	0.04	0.14	0.14	0.14
4	0.16	0.16	0.16	0.2	0.24	0.28
5	0.22	0.2	0.1	0.26	0.3	0.4
6	0.28	0.12	0.28	0.32	0.16	0.34
7	0.34	0.3	0.3	0.38	0.42	0.38
8	0.4	0.42	0.34	0.44	0.12	0.22
9	0.44	0.48	0.12	0.5	0.18	0.46
10	0.5	0.5	0.5	0.06	0.06	0.36

6.2 Discussion of damage severities evaluation

To evaluate the damage severity, the beams with ten different severity combinations specified by various magnitudes of α, presented in Table 4, are considered. The GA is applied with the proposed fitness function to calculate the damage severity. Figure 9 shows the search convergence process for different damage scenarios. The results of the damage severity detection of beam 1 for each damage case are shown in Table 5 and Fig. 9a. It can be observed from the histograms that the proposed algorithm precisely follows the corresponding specified crack location and severity for the damage cases.

More difficult cases are encountered in multiple damage scenarios with different severities as in beams 2 and 3. Beam 2 relates to two points of damage whose depths are different in each case. Beam 3 has three points of damage, which simulates an even more complicated damage scenario due to the variety of depth values. To show the robustness and sensitivity of the proposed algorithm, the GA is assigned to obtain the damage severity in the specified locations. Table 5 presents the predicted value of damage severities. As shown in Fig. 9b, c, estimation of the proposed algorithm accurately follows the corresponding values.

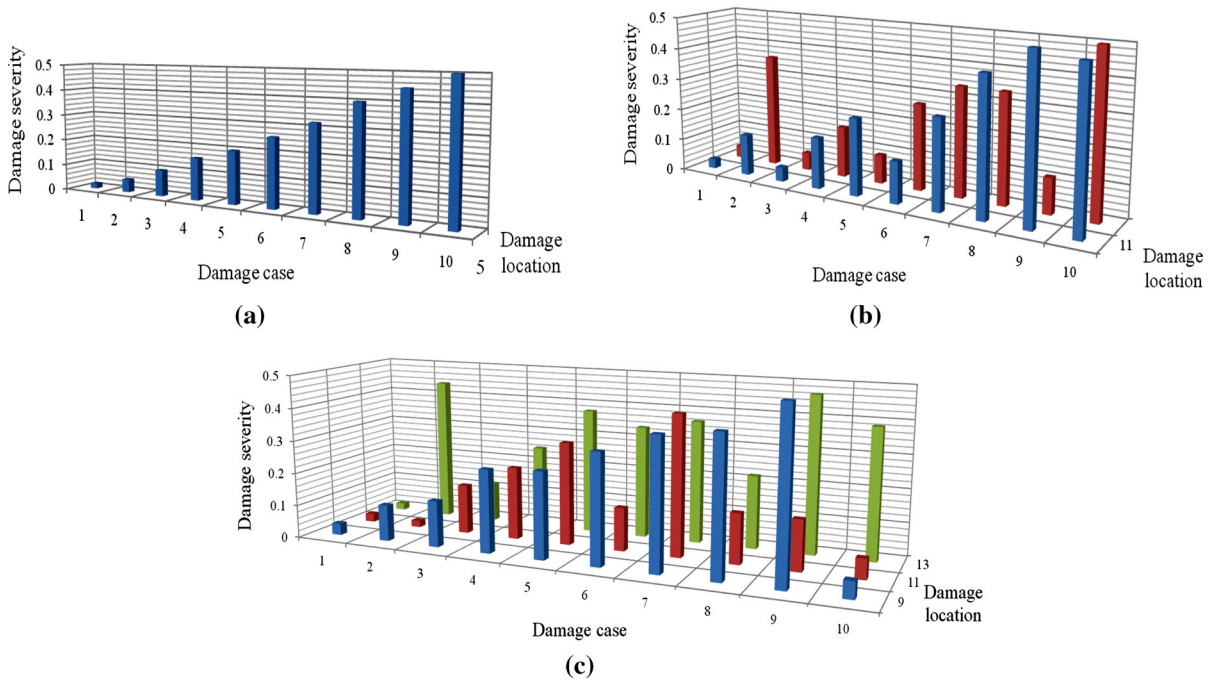

Fig. 9 The damage severity evaluation results by using GA. **a** Beam 1, **b** beam 2, **c** beam 3

The evaluation errors for severities of damages in beams 1 and 2 are in the range of 0–6 % with mean values of 1.20, 2.00 and 2.20 %. Also, with the increase of damage severities in beam 3, the prediction errors vary in an acceptable range from 0 to 8 % with mean values of 2.20, 3.00 and 2.60 %. Therefore, the proposed algorithm is effective in evaluating the damage severities and yields reasonably good results when the data contain a certain level of noise.

7 Experimental verification

To verify the effectiveness of the proposed method, an experimental study is carried out on a test beam. Most of the vibration-based damage identification techniques obtained from the measured signals requires modal properties, which are sensitive to measurement error and noise. The proposed damage identification technique has to be validated using real measurement data from vibration tests in the presence of measurement errors and noise. Vibration tests are carried out on four I-section steel beams with a span length of 3 m, as depicted in Fig. 10, under undamaged and various damage states. The damage is induced by introducing a saw cut at the prescribed locations on the beam with varying depths of cut, as described in Table 6.

The analogue data from the sensors is converted via an analysis digital center using the OROS OR35 analyzer. The signal analyzer is capable of generating all the different forms of signals, including white noise, which is used in this test. The beam is excited using a shaker at node 14. The acceleration response of the K-shear Kistler accelerometers is measured at sixteen locations on the top flange along the beam (Fig. 10b). These accelerometers have a frequency range of 0.5–10 kHz and a sensitivity of 100 mV/g. The sampling rate is set to 5.12 kS/s to achieve the frequency band width of 2000 Hz.

7.1 Experimental results

For evaluation of the location of damage through the measured acceleration responses, the RWPE is implemented for each considered beam as shown in Fig. 11. It is observed that the damage location in beam 1 can be precisely identified with DB2 and decomposition level 6 based on the change of RWPE values shown in Fig. 11a. In beam 2, DB 5 with 6 levels of

Table 5 The damage severity results obtained by GA

Case	Predicted value						Error (%)					
	Beam 1	Beam 2		Beam 3			Beam 1	Beam 2		Beam 3		
	α_1^*	α_1^*	α_2^*	α_1^*	α_2^*	α_3^*	ε_1^a	ε_1^a	ε_2^b	ε_1^a	ε_2^b	ε_3^c
1	0.02	0.02	0.04	0.04	0.02	0.02	0	0	2	2	2	0
2	0.06	0.14	0.34	0.12	0.02	0.42	2	4	6		0	6
3	0.1	0.04	0.06	0.14	0.16	0.1	0	2	2	0	2	4
4	0.16	0.16	0.16	0.26	0.2	0.24	0	0	0	6	4	4
5	0.2	0.26	0.08	0.26	0.32	0.36	2	6	2	0	2	4
6	0.24	0.14	0.26	0.34	0.1	0.34	4	2	2	2	6	0
7	0.32	0.26	0.34	0.4	0.42	0.36	2	4	4	2	0	2
8	0.4	0.42	0.34	0.4	0.2	0.22	0	0	0	4	8	0
9	0.46	0.5	0.1	0.5	0.12	0.48	2	2	2	0	6	2
10	0.5	0.48	0.5	0.04	0.06	0.4	0	2	0	2	0	4
Mean error							1.20	2.20	2.00	2.20	3.00	2.60

[a] The detection error, $\varepsilon_1 = \left|\alpha_1^* - \alpha_1\right| \times 100\,\%$

[b] The detection error, $\varepsilon_2 = \left|\alpha_2^* - \alpha_2\right| \times 100\,\%$

[c] The detection error, $\varepsilon_3 = \left|\alpha_3^* - \alpha_3\right| \times 100\,\%$

Fig. 10 Dynamic test in laboratory. **a** Damage locations of tested beams, **b** data acquisition system

decomposition is chosen for the two-damage scenarios, since the damage locations presented in Fig. 11b are distinguishable in these histograms with RWPE reaching a peak value at locations 11 and 13. Moreover, location 11 has a relatively larger damage index while location 13 has a comparatively lower RWPE. The reason lies in the damage location, which is adjacent to the support. It should be mentioned that selection of a non-suitable type of wavelet may causes a false-negative indication.

A similar trend of damage index, as in beam 2, is observed for beam 3 by using DB10 and decomposition level 6 with three damage locations at points 9, 11 and 13, as shown in Fig. 11c. Evaluation of the RWPE

Table 6 Damage scenarios

Damage case	Damage scenario	Damage location	Width of damage (mm)	Depth of damage (mm)
Beam 0	Undamaged	–	–	–
Beam 1	Single	5	3	3 up to 75
Beam 2	Double	11, 13	3	3 up to 75
Beam 3	Triple	9, 11, 13	3	3 up to 75

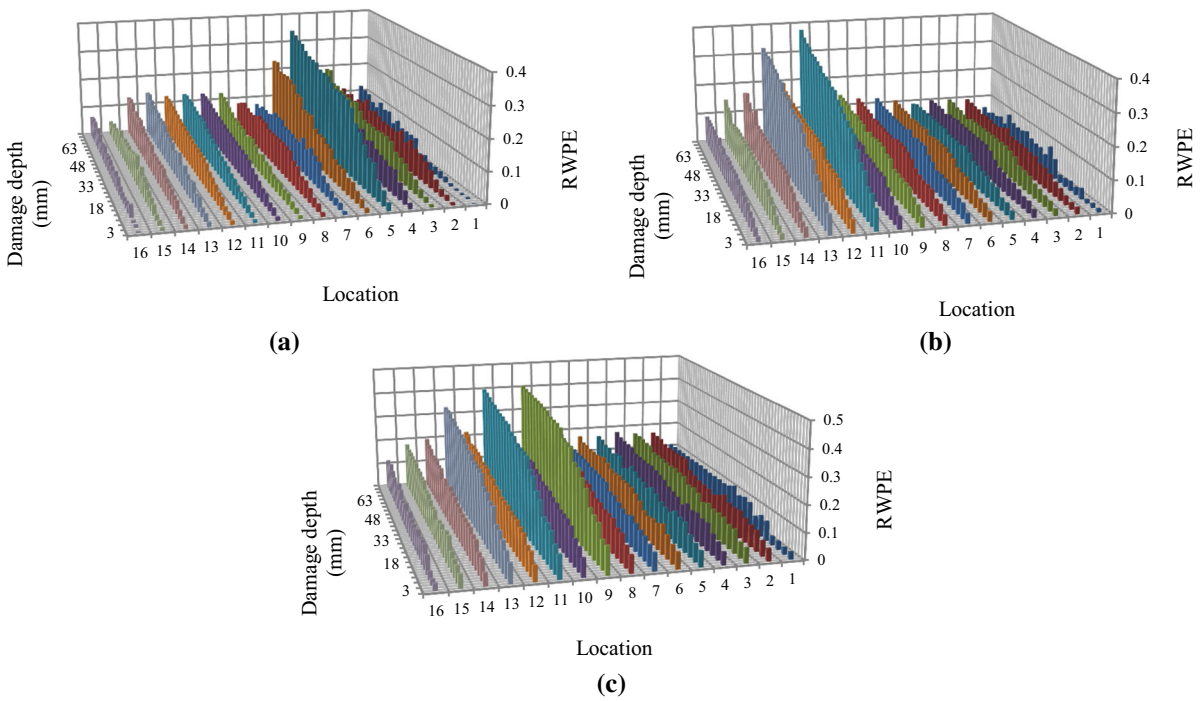

Fig. 11 RWPE for different damage cases. **a** Beam 1, **b** beam 2, **c** beam 3

associated with beam 3 shows the damage locations precisely with respect to the support, as mentioned earlier for beam 2.

The presented results demonstrate that the proposed damage index (RWPE) can identify the damage location accurately in all damage scenarios from the dynamic measurement. In addition, varying operational and environmental conditions of the structure raise a discrepancy, i.e., false alarm, which can be reduced by choosing an appropriate mother wavelet function and decomposition level.

After identification of the damage locations, the analysis evaluates the severity of the damage. The optimization algorithm presented in Sect. 6.1 is employed for detection of the severity of damage. All of the considered beams with different damage scenarios and various levels of severity are subjected to damage severity detection by the proposed algorithm where α is varied from 0.02 to 0.5 with the step length of 0.02. The detection results for each damage scenario of the GA are found to be accurate and identical to the real values of severity. For instance, the results of GA encoded as a binary number associated with case 3 with three depth ratios of $\alpha_{23} = 0.46$, $\alpha_9 = 0.46$ and $\alpha_{25} = 0.5$ are shown in Fig. 12.

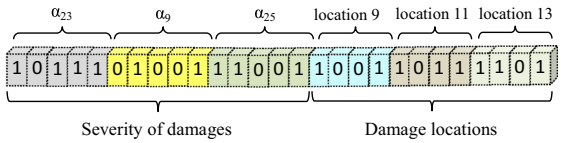

Fig. 12 Encoded damage severity result for beam 3 with different levels of severity

8 Conclusions

A two-step vibration-based damage detection method is proposed to determine the location and severity of damage in beam structures. The damage locations are accurately identified in the first step by proposing a new damage index based on the WPT, which is combined with the information entropy to take advantage of both techniques. Based on the results it can be concluded that the selections of a proper mother wavelet function and decomposition level are crucial to improve the performance of the proposed algorithm. On the other hand, the wavelet-based techniques are absolutely dependent on the mother wavelet function, whose correlation with the signal is influenced by the locations and number of points of damages. It should be highlighted that utilization of a specific mother wavelet and a decomposition level does not necessarily successfully identify various damage scenarios that are located on a beam. Once the damages are located, the severity evaluation database is defined in terms of the relationships between the component energies and the damage severities. The GA optimization is then used to evaluate the damage severities by exploring the database. The effectiveness of the proposed method is examined by both numerical simulation and experimental tests. Sensitivity and robustness of the method is then tested against noise-contaminated signal. The results show that the proposed algorithm can accurately identify the locations of damage as well as the damage severity even for multiple-damage scenarios.

Although the proposed damage identification methodology has shown great potential in the simulated and the laboratory tested beam, the proper selection of mother wavelet functions and decomposition levels are determined by trial-and-error based on the intrinsic properties of the data. Further work is needed to apply the computational intelligence methods to optimize the algorithm so as to determine the best values for "mother wavelet function" and "decomposition level of the signals by means of wavelet analysis". These are practical aspects that should be studied further so that a RWPE-based structural damage identification method can be applied with confidence to real structures.

Acknowledgments The authors would like to express their sincere thanks to the Ministry of Education, Malaysia for the support given through research Grants FP027/2012A and UM.C/625/1/HIR/MOHE/ENG/55.

References

1. Doebling SW, Farrar CR, Prime MB (1998) A summary review of vibration-based damage identification methods. Shock Vib Dig 30(2):91–105
2. Carden EP, Fanning P (2004) Vibration based condition monitoring: a review. Struct Health Monit 3(4):355–377
3. Sohn H, Farrar CR, Hemez FM, Shunk DD, Stinemates DW, Nadler BR, Czarnecki JJ (2004) A review of structural health monitoring literature: 1996–2001. Los Alamos National Laboratory Report, LA-13976-MS
4. Yan Y, Cheng L, Wu Z, Yam L (2007) Development in vibration-based structural damage detection technique. Mech Syst Signal Process 21(5):2198–2211
5. Fan W, Qiao P (2011) Vibration-based damage identification methods: a review and comparative study. Struct Health Monit 10(1):83–111
6. Doherty JE (1987) Nondestructive evaluation. In: Kobayashi AS (ed) Handbook on experimental mechanics. Society for Experimental Mechanics Inc, Bethel
7. Chang PC, Liu SC (2003) Recent research in nondestructive evaluation of civil infrastructures. J Mater Civ Eng 15(3):298–304
8. Gabor D (1946) Theory of communication. IEEE J 21:149–157
9. Kim BH, Park T, Voyiadjis GZ (2006) Damage estimation on beam-like structures using the multi-resolution analysis. Int J Solids Struct 43(14):4238–4257
10. Taha MR, Noureldin A, Lucero J, Baca T (2006) Wavelet transform for structural health monitoring: a compendium of uses and features. Struct Health Monit 5(3):267–295
11. Jiang X, Mahadevan S (2011) Wavelet spectrum analysis approach to model validation of dynamic systems. Mech Syst Signal Process 25(2):575–590
12. Melhem H, Kim H (2003) Damage detection in concrete by fourier and wavelet analyses. J Eng Mech 129(5):571–577
13. Kim H, Melhem H (2003) Fourier and wavelet analyses for fatigue assessment of concrete beams. Exp Mech 43(2):131–140
14. Salehian A, Hou Z, Yuan FG (2003) Identification of location of a sudden damage in plates using wavelet approach. In: Proceedings of 16th ASCE engineering mechanics conference, University of Washington, Seattle, WA, USA, 16–18 July 2003

15. Gentile A, Messina A (2003) On the continuous wavelet transforms applied to discrete vibrational data for detecting open cracks in damaged beams. Int J Solids Struct 40(2):295–315
16. Loutridis S, Douka E, Trochidis A (2004) Crack identification in double-cracked beams using wavelet analysis. J Sound Vib 277(4):1025–1039
17. Chang C-C, Chen L-W (2005) Detection of the location and size of cracks in the multiple cracked beam by spatial wavelet based approach. Mech Syst Signal Process 19(1):139–155
18. Castro E, Garcia-Hernandez M, Gallego A (2006) Damage detection in rods by means of the wavelet analysis of vibrations: influence of the mode order. J Sound Vib 296(4):1028–1038
19. Rucka M, Wilde K (2006) Application of continuous wavelet transform in vibration based damage detection method for beams and plates. J Sound Vib 297(3):536–550
20. Spanos PD, Failla G, Santini A, Pappatico M (2006) Damage detection in Euler–Bernoulli beams via spatial wavelet analysis. Struct Control Health Monit 13(1):472–487
21. Zhong S, Oyadiji S (2007) Crack detection in simply supported beams without baseline modal parameters by stationary wavelet transform. Mech Syst Signal Process 21(4):1853–1884
22. Gökdağ H, Kopmaz O (2009) A new damage detection approach for beam-type structures based on the combination of continuous and discrete wavelet transforms. J Sound Vib 324(3):1158–1180
23. Zhong S, Oyadiji SO (2011) Detection of cracks in simply-supported beams by continuous wavelet transform of reconstructed modal data. Comput Struct 89(1):127–148
24. Jiang X, Ma ZJ, Ren WX (2012) Crack detection from the slope of the mode shape using complex continuous wavelet transform. Comput Aided Civ Infrastruct Eng 27(3):187–201
25. Nikravesh SMY, Chegini SN (2013) Crack identification in double-cracked plates using wavelet analysis. Meccanica 48(9):2075–2098
26. Zhong S, Oyadiji SO (2013) Sampling interval sensitivity analysis for crack detection by stationary wavelet transform. Struct Control Health Monit 20(1):45–69
27. Wang Q, Deng X (1999) Damage detection with spatial wavelets. Int J Solids Struct 36(23):3443–3468
28. Umesha P, Ravichandran R, Sivasubramanian K (2009) Crack detection and quantification in beams using wavelets. Comput Aided Civ Infrastruct Eng 24(8):593–607
29. Quek S, Wang Q, Zhang L, Ong K (2001) Practical issues in the detection of damage in beams using wavelets. Smart Mater Struct 10 (5):1009
30. Sun Z, Chang C (2004) Statistical wavelet-based method for structural health monitoring. J Struct Eng 130(7):1055–1062
31. Han J-G, Ren W-X, Sun Z-S (2005) Wavelet packet based damage identification of beam structures. Int J Solids Struct 42(26):6610–6627
32. Ding Y, Li A, Liu T (2008) A study on the WPT-based structural damage alarming of the ASCE benchmark experiments. Adv Struct Eng 11(1):121–127
33. Hu WB, Hu W, Zheng Y (2010) Wavelet analysis in damage detection for bridge structure. Key Eng Mater 417:813–816
34. Tabrizi A, Garibaldi L, Fasana A, Marchesiello S (2014) Early damage detection of roller bearings using wavelet packet decomposition, ensemble empirical mode decomposition and support vector machine. Meccanica. doi:10.1007/s11012-014-9968-z
35. Ravanfar SA, Razak HA, Ismail Z, Hakim S (2014) Damage Detection Based on Wavelet Packet Transform and Information Entropy. In: Proceedings of the 32nd IMAC, a conference and exposition on structural dynamics, Florida, USA, 3–6 Feburary 2014, pp 223–229
36. Yun GJ, Lee S-G, Carletta J, Nagayama T (2011) Decentralized damage identification using wavelet signal analysis embedded on wireless smart sensors. Eng Struct 33(7):2162–2172
37. Lee S, Yun G, Shang S (2014) Reference-free damage detection for truss bridge structures by continuous relative wavelet entropy method. Structural Health Monitoring. doi:10.1177/1475921714522845
38. Ren W-X, Sun Z-S (2008) Structural damage identification by using wavelet entropy. Eng Struct 30(10):2840–2849
39. Rosso O, Martin M, Figliola A, Keller K, Plastino A (2006) EEG analysis using wavelet-based information tools. J Neurosci Methods 153(2):163–182
40. Haupt RL, Haupt SE (2004) Practical genetic algorithms. Wiley, New Jersey
41. Panigrahi S, Chakraverty S, Mishra B (2009) Vibration based damage detection in a uniform strength beam using genetic algorithm. Meccanica 44(6):697–710
42. Perera R, Ruiz A, Manzano C (2009) Performance assessment of multicriteria damage identification genetic algorithms. Comput Struct 87(1):120–127
43. Perera R, Fang S-E, Ruiz A (2010) Application of particle swarm optimization and genetic algorithms to multiobjective damage identification inverse problems with modelling errors. Meccanica 45(5):723–734
44. Mehrjoo M, Khaji N, Ghafory-Ashtiany M (2013) Application of genetic algorithm in crack detection of beam-like structures using a new cracked Euler-Bernoulli beam element. Appl Soft Comput 13(2):867–880
45. Hao H, Xia Y (2002) Vibration-based damage detection of structures by genetic algorithm. J Comput Civ Eng 16(3):222–229
46. Vakil-Baghmisheh M-T, Peimani M, Sadeghi MH, Ettefagh MM (2008) Crack detection in beam-like structures using genetic algorithms. Appl Soft Comput 8(2):1150–1160
47. Wang Y, Chen X, He Y, He Z (2010) New decoupled wavelet bases for multiresolution structural analysis. Struct Eng Mech 35(2):175–190
48. Mallat SG (1989) A theory for multiresolution signal decomposition: the wavelet representation. IEEE Trans Pattern Anal Mach Intell 11(7):674–693
49. Ovanesova A, Suarez L (2004) Applications of wavelet transforms to damage detection in frame structures. Eng Struct 26(1):39–49
50. Shinde A, Hou Z (2005) A wavelet packet based sifting process and its application for structural health monitoring. Struct Health Monit 4(2):153–170
51. Mikami S, Beskhyroun S, Oshima T (2011) Wavelet packet based damage detection in beam-like structures without baseline modal parameters. Struct Infrastruct Eng 7(3):211–227

52. Sun Z, Chang C-C (2007) Vibration based structural health monitoring: wavelet packet transform based solution. Struct Infrastruct Eng 3(4):313–323
53. Neild S, McFadden P, Williams M (2003) A review of time-frequency methods for structural vibration analysis. Eng Struct 25(6):713–728
54. Mallat S (1999) A wavelet tour of signal processing, 2nd edn. Academic press, New York
55. Yen GG, Lin K-C (2000) Wavelet packet feature extraction for vibration monitoring. IEEE Trans Ind Electron 47(3):650–667
56. Law S, Li X, Zhu X, Chan S (2005) Structural damage detection from wavelet packet sensitivity. Eng Struct 27(9):1339–1348
57. Ren W-X, Sun Z-S, Xia Y, Hao H, Deeks AJ (2008) Damage identification of shear connectors with wavelet packet energy: laboratory test study. J Struct Eng 134(5):832–841
58. He Y, Guo D, Chu F (2001) Using genetic algorithms and finite element methods to detect shaft crack for rotor-bearing system. Math Comput Simul 57(1):95–108